ARTICLE IN PRESS

Magnetic Resonance Letters xxx (xxxx) xxx

KeA1
CHINESE ROOTS
GLOBAL IMPACT

Contents lists available at ScienceDirect

Magnetic Resonance Letters

journal homepage: www.keaipublishing.com/MRL



On the use of residual dipolar couplings in multi-state structure calculation of two-domain proteins

Alexandra Born ^a, Morkos A. Henen ^{a, b}, Parker J. Nichols ^a, Beat Vögeli ^{a, *}

ARTICLE INFO

Article history: Received 29 September 2021 Received in revised form 21 October 2021 Accepted 24 October 2021 Available online xxx

Keywords: RDC Residual dipolar coupling Two-domain protein Multi-state structure

ABSTRACT

Residual dipolar couplings (RDCs) are powerful nuclear magnetic resonance (NMR) probes for the structure calculation of biomacromolecules. Typically, an alignment tensor that defines the orientation of the entire molecule relative to the magnetic field is determined either before refinement of individual bond vectors or simultaneously with this refinement. For single-domain proteins this approach works well since all bond vectors can be described within the same coordinate frame, which is given by the alignment tensor. However, novel approaches are sought after for systems where no universal alignment tensor can be used. Here, we present an approach that can be applied to two-domain proteins that enables the calculation of multiple states within each domain as well as with respect to the relative positions of the two domains.

© 2021 The Authors. Publishing services by Elsevier B.V. on behalf of KeAi Communications Co. Ltd. This is an open access article under the CC BY license (http://creativecommons.org/licenses/by/4.0/).

1. Introduction

The majority of proteins contain more than one domain. Spatial sampling between the domains may be important for the function and is typically on much larger scale than within the domains [1,2]. However, it is not trivial to reconstruct such dynamics from time-averaged structural nuclear magnetic resonance (NMR) probes [3–7].

We have recently introduced a novel method to solve the multi-state structure of a two-domain protein that allows for coupling between intra- and interdomain sampling [8]. To that purpose, we derived structural restraints from exact NOEs [9–11], scalar couplings [12], paramagnetic relaxation enhancements (PREs) [5,13,14], and residual dipolar couplings (RDCs) [15–17], all of which are averaged over milliseconds and must be fulfilled by all structural states together rather than individually. While it is simple to calculate multi-state structural ensemble for each domain alone, it is difficult to allow for multiple positions and orientations of the domains relative to one another in a calculation including both domains. As previously established for single-domain proteins [18], we apply bundling restraints [19] during multi-state calculation to prevent that individual states stray further apart than required by the experimental restraints. However, such restraints cannot be applied to both domains simultaneously when they undergo large relative motion. Therefore, we calculate a structural ensemble for one domain first using only restraints relevant for that domain. In a second step, we apply all

E-mail address: beat.vogeli@cuanschutz.edu (B. Vögeli).

https://doi.org/10.1016/j.mrl.2021.10.003

2772-5162/© 2021 The Authors. Publishing services by Elsevier B.V. on behalf of KeAi Communications Co. Ltd. This is an open access article under the CC BY license (http://creativecommons.org/licenses/by/4.0/).

Please cite this article as: A. Born, M.A. Henen, P.J. Nichols et al., On the use of residual dipolar couplings in multi-state structure calculation of two-domain proteins, Magnetic Resonance Letters, https://doi.org/10.1016/j.mrl.2021.10.003

^a University of Colorado Anschutz Medical Campus, Department of Biochemistry and Molecular Genetics, 12801 East 17th A Venue, Aurora, CO, 80045, USA

^b Faculty of Pharmacy, Mansoura University, Mansoura, 35516, Egypt

^{*} Corresponding author. Department of Biochemistry and Molecular Genetics, University of Colorado Denver, Research Center 1 South, Room 9103, 12801 East 17th Avenue, Aurora, CO, 80045, USA.

restraints to the entire protein but apply the bundling restraints only to the second domain, while we freeze all angles of the individual states of the first domain. This way, we only let the entire first domain move relative to the second domain during structure calculation.

This protocol poses a particular challenge for the use of the RDCs in the second structural calculation step. In the first step, we simply use an alignment tensor fitted to the first domain and use the RDCs in a standard manner. For the second step, we use the alignment tensor fitted to the second domain. If the domains tumble relatively independently, this tensor is different from the first. It is straightforward to use the second tensor for refinement of the second domain. However, RDCs also report on the relative domain sampling because they depend on the bond orientation within molecule-fixed frames and thus carry long-range information. Therefore, we use the RDCs of the first domain also in the second step of the calculation. In this communication, we provide the theoretical basis for our procedure.

2. Theory

A set of RDCs D_i between atom types a and b obtained from a single-domain protein can be described by an alignment tensor valid for each RDC [16]:

$$D_{i} = K \sum_{q=-2}^{+2} \left\langle Y^{*}_{2q} \left(\theta_{i}(t), \varphi_{i}(t) \right) Y_{2q} \left(\zeta_{dom}(t), \xi_{dom}(t) \right) \right\rangle$$

$$\tag{1}$$

where Y_{2q} are the second rank spherical harmonics with q = -2, ..., +2. We assume that the fluctuations of the interatomic distances are not correlated with their orientations such that they can be treated as constants given by effective distances r_i^{eff} absorbing fluctuations in a uniform manner for all RDCs. Therefore, the constant K is given by

$$K = -\left(\frac{\mu_0}{4\pi}\right) \frac{\gamma_a \gamma_b \hbar}{\pi \left(r_i^{eff}\right)^3} \tag{2}$$

with μ_0 the permeability of free space, γ the gyromagnetic ratios of atoms a and b, and \hbar Planck's constant. The polar angles ζ_{dom} and ξ_{dom} effectively transform the laboratory frame into a molecule-fixed frame and describe the overall alignment of the domain as a function of time t, and likewise θ_i and φ_i give the orientations of the a-b interatom vectors with respect to the overall orientation. The brackets <> indicate time and ensemble averaging.

Because all sampled conformations of the molecule can be assumed to be similar, the averaging can be carried out independently for the two factors:

$$D_{i} = K \sum_{q=-2}^{+2} \left\langle Y^{*}_{2q} \left(\theta_{i}(t), \varphi_{i}(t) \right) \right\rangle \left\langle Y_{2q} \left(\zeta_{dom}(t), \xi_{dom}(t) \right) \right\rangle$$
(3)

The averaged spherical harmonics of angles ζ_{dom} and ξ_{dom} are usually written as a vector \overrightarrow{A} consisting of five elements and is referred to as 'alignment tensor', and obtained in a fit that simultaneously yields all θ_i and φ_i (with some redundancy) or fitted to a known structure (e.g., singular value decomposition, SVD [20]).

For technical reasons (see below), we apply structural restraints in two-domain proteins in two separate steps for the two domains if more than one conformation ('state') is allowed to fulfill the restraints on average (in particular, bundling restraints cannot be applied to both domains simultaneously when the domains are supposed to sample very different positions relative to one another). Although it is theoretically possible to apply all RDC restraints in one calculation (e.g., in the second step), we use the following approach to apply RDC restraints with different alignment tensors in the two structure calculation steps. We assume that domain A is more restricted under alignment conditions. Typically, this is the larger domain. Our approach is to first carry out a structure calculation on the less aligned domain B. The RDC restraints *j* that only include RDCs from domain B, are used with a domain B-specific alignment tensor (we use a tilde to designate that these angles are expressed in the B frame):

$$D_{j}^{domB} = K \sum_{q=-2}^{+2} \langle Y^*_{2q}(\tilde{\theta}_{j}(t), \tilde{\varphi}_{j}(t)) \rangle \langle Y_{2q}(\zeta_{domB}(t), \xi_{domB}(t)) \rangle$$

$$\tag{4}$$

In the second step, the structure of domain B is frozen by fixing its torsion angles. The structure calculation is then applied to the entire molecule, using the restraints of both domains A and B, where the domain A, and possibly a linker, have the usual

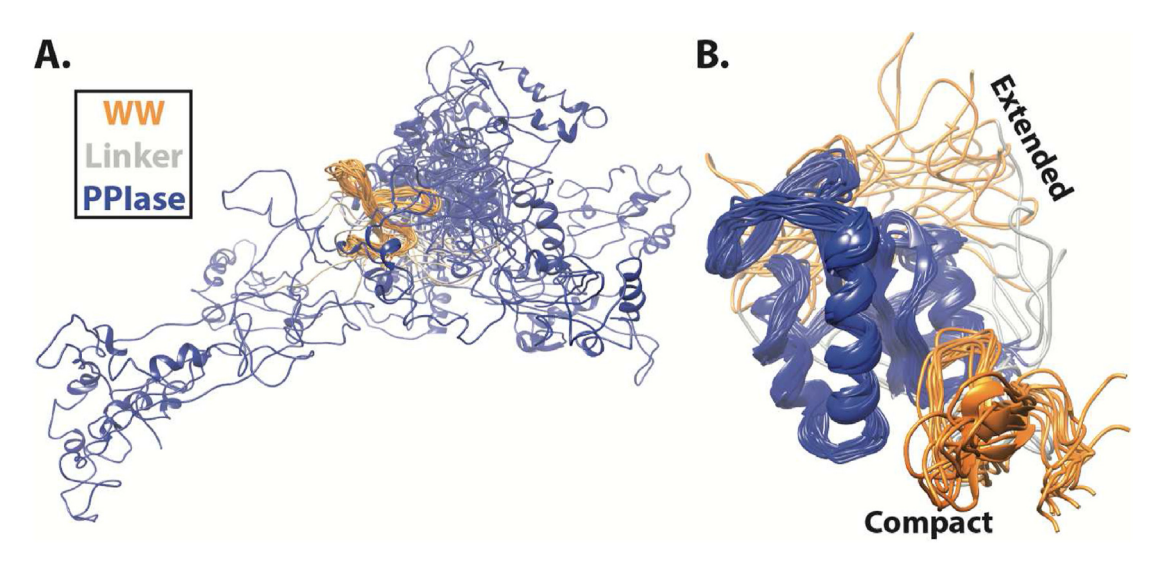


Fig. 1. Two-state structure of Pin1. A) Two-state structural ensemble after calculation step 1 with WW overlaid. B) Extended and compact Pin1 with PPlase overlaid to show the relative position of the WW domain after step 2.

degrees of freedom. Therefore, the only degrees of freedom associated with domain B are given by its position relative to domain A. The RDCs restraining domain A, k, are used analogously to equation (3):

$$D_{k}^{domA} = K \sum_{q=-2}^{+2} \langle Y^{*}_{2q} (\theta_{k}(t), \varphi_{k}(t)) \rangle \langle Y_{2q} (\zeta_{domA}(t), \xi_{domA}(t)) \rangle$$
(5)

where the alignment tensor is the one specific for domain A.

Following equation (1), the RDCs for domain B in the second step can be expressed as (note, we do not use the separate averaging from equation (4) anymore at this point):

$$D_{j}^{domB} = K \sum_{q=-2}^{+2} \langle Y^*_{2q}(\tilde{\theta}_{j}(t), \tilde{\varphi}_{j}(t)) Y_{2q}(\zeta_{domB}(t), \xi_{domB}(t)) \rangle$$

$$(6)$$

Next, we seek to express the RDC restraints on domain B also in dependence of alignment tensor of domain A. We use the Wigner rotation elements $D_{qq'}^{(2)}$ to apply an additional frame change:

$$D_{j}^{domB} = K \sum_{q,q'=-2}^{+2} \left\langle Y^{*}_{2q} \left(\tilde{\theta}_{j}(t), \tilde{\varphi}_{j}(t) \right) D_{qq'}^{(2)} \left(\Omega(t) \right) Y_{2q'} \left(\zeta_{domA}(t), \xi_{domA}(t) \right) \right\rangle$$

$$(7)$$

We designate the time-dependent angles that relate the A and B domain-fixed frames collectively Ω . Analogously to equation (3), we use a separate averaging of the last factor:

$$D_{j}^{domB} = K \sum_{q,q'=-2}^{+2} \left\langle Y^{*}_{2q} \left(\tilde{\theta}_{j}(t), \tilde{\varphi}_{j}(t) \right) D_{qq'}^{(2)} \left(\Omega(t) \right) \right\rangle \left\langle Y_{2q'} \left(\zeta_{domA}(t), \xi_{domA}(t) \right) \right\rangle$$
(8)

This is only strictly true if the alignment of domain A is independent of the time dependence of Ω . Importantly, this does not require the relative position of domain B with respect to domain A not to have any impact. It only requires that the impact is the same at all relative positions. We also note that this condition is caused by the fact that the timescale of relative domain reorientation (typically micro-to milliseconds) is slower than the alignment timescale (nanoseconds).

reorientation (typically micro-to milliseconds) is slower than the alignment timescale (nanoseconds). Using $\sum_{q=-2}^{+2} Y^*_{2q}(\tilde{\theta}_j(t), \tilde{\varphi}_j(t)) D_{qq'}^{(2)}(\Omega(t)) = Y^*_{2q'}(\theta_j(t), \varphi_j(t))$, the RDCs in domain B can now expressed by angles defined in frame A:

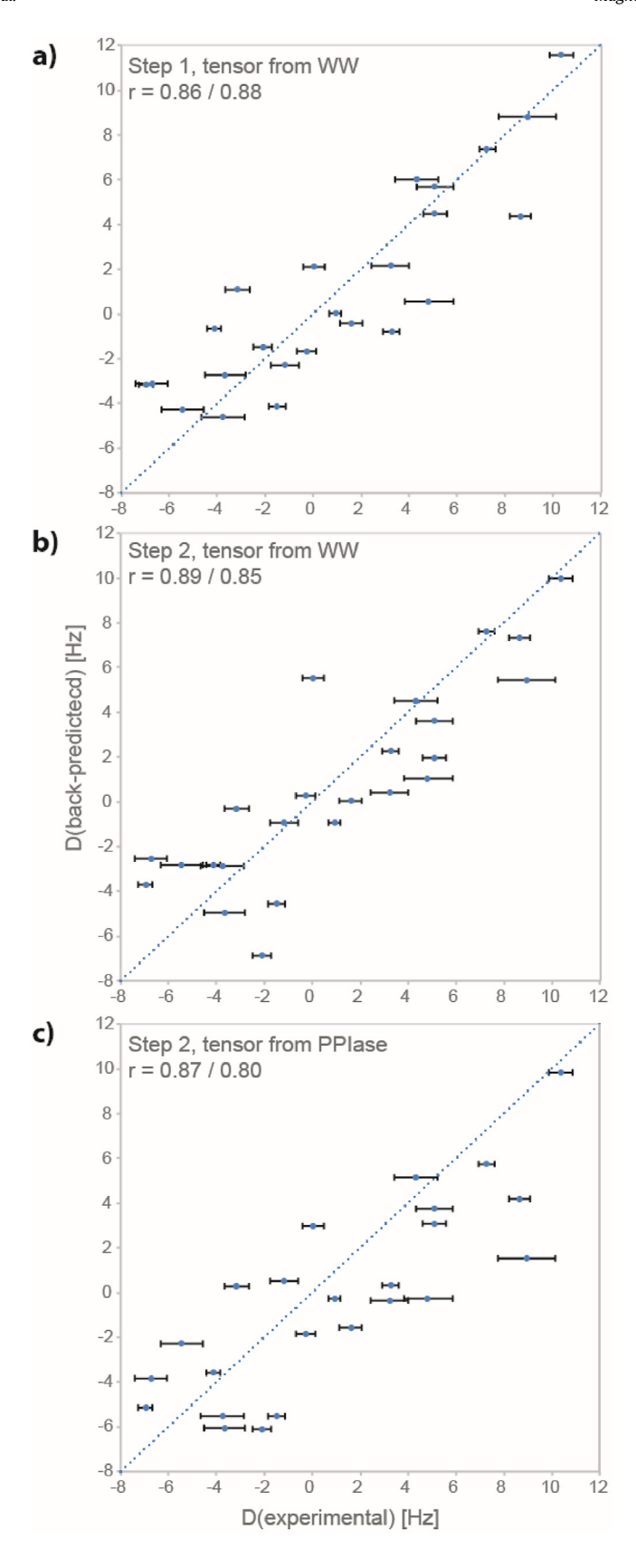


Table 1Two-state structure calculation of Pin1.

| | Step 1 | Step 2 |
|--|---|--|
| Bundling restraints | WW domain | PPIase domain |
| Frozen structure | _ | WW domain |
| RDC alignment tensor, magnitude ^a , rhombicity ^a , restrained residues | WW domain, -6.535 Hz, 0.449, WW domain residues | PPlase domain, 16.46 Hz, 0.242, all residues |
| Interdomain restraints | _ | PREs, interdomain NOEs |
| Intradomain restraints | WW domain ^b | all |
| number of lowest TF structures used | 20 | 10 |
| Ave TF [Å ²] | 99.08 | 148.30 |
| SD TF [Å ²] | 0.91 | 3.89 |
| WW RMSD ^c [Å] | 1.05 (0.82) | 0.90 (0.75) |
| PPIase RMSD ^c [Å] | | 0.94 (0.73) |

a determined using the "FindTensor" script in CYANA using 6svc and 1Pin for WW and PPIase domain, respectively, where $D_i = \text{magnitude } \{3\cos^2(\theta_i) - 1 + 3/2 \text{*rhombicity*} \sin^2(\theta_i)\cos(2\phi_i)\}$; the CYANA-specific magnitude and rhombicity relate to the 5x1 alignment vector $\langle Y_{2q} \rangle_{q} = \{-2, \dots, +2\}$ as follows: magnitude $= A_z/2$ and rhombicity $= 2/3 \text{*} (A_x - A_y)/A_z$, where $A_{x,y,z}$ are the Eigenvalues of the 3x3 Saupé Matrix constructed from $\langle Y_{2q} \rangle$.

$$D_{j}^{domB} = K \sum_{q'=-2}^{+2} \langle Y^{*}_{2q'}(\theta_{j}(t), \varphi_{j}(t)) \rangle \langle Y_{2q'}(\zeta_{domA}(t), \xi_{domA}(t)) \rangle$$

$$(9)$$

Although the RDC orientation vector are fixed within frame B, and therefore with respect to one another, the structure calculation will modify the θ_i and the φ_i angles, which is equivalent to finding a solution for $D_{\alpha g'}^{(2)}$.

3. Practical

We applied the approach to Pin1, a two-domain protein that isomerizes prolines preceded by a phosphorylated serine or threonine (pS/TP) [21,22]. Residues 1–39 form the WW domain comprising a three-stranded, antiparallel β -sheet which binds the pS/TP motif *trans*-specifically [23]. Residues 50–163 form the PPlase domain composed of a four-stranded core β -sheet with four exterior α -helices and responsible for the proline isomerization in the same motif [24]. A ten-residue flexible linker between the two domains allows them to tumble partially independently [25–28]. Pin1 mainly samples compact and extended states with populations of ~70% and ~30%, respectively [8].

Using C12E5 PEG/hexanol as alignment medium, we measured 478 RDCs ($140^{1}D_{\text{Ni,HNi}}$, $138^{1}D_{\text{Ci,Czi}}$, $103^{1}D_{\text{Ci,Ni+1}}$, and 97 $D_{\text{Ci,HNi+1}}$) for Pin1 [8]. We determined the alignment tensors using the "FindTensor" CYANA [29] script to perform a singular value decomposition (SVD) using the structures 6svc [30] (single-state eNOE structure of the isolated WW domain; Pearson's correlation coefficient r = 0.94) and 1 pin [31] (X-ray structure; r = 0.92, after removal of outliers 0.96) for the WW and PPlase domain, respectively. The WW tensor has a magnitude of -6.535 Hz with rhombicity of 0.449 (as defined in CYANA, see Table 1), while the PPlase tensor yields 16.46 Hz and 0.242, respectively. During structure calculation, CYANA keeps these parameters fixed, but allows the tensor to reorient.

To calculate two-state structural ensembles in CYANA-3.98²⁹, we followed the previously described protocol [8]. In addition to the RDCs, we used 2268 eNOE-, 1937 gnNOE- [32], 20 interdomain NOE-, and 250 interdomain PRE distance restraints, and 265 scalar coupling- and 66 chemical shift-based dihedral angle restraints. Due to the bundling restraints needed to solve a multi-state structure, a two-step calculation was performed to allow the domains to sample various positions. In the first step, only the WW domain experimental and bundling restraints have to be used (optionally, the intradomain restraints without bundling restraints can be additionally applied to the PPIase domain, which we did for the current calculation), and in the second step we applied only the PPIase domain bundling restraints but all experimental restraints. In step 1, we used the WW alignment tensor fitted using the WW domain RDCs. The 10 calculations with the lowest target function (TF; proportional to the sum of squared violations) were then used as input for the second calculation. After fixing all dihedral angles in the WW domain, all experimental restraints and bundling restraints for the PPIase domain were used in step 2, such that the orientation of the WW domain relative to the PPIase domain is determined by the interdomain PREs, interdomain NOEs, and the RDCs. Importantly, the RDC alignment tensor for step 2 is based on the PPIase domain, but RDCs

b We also applied the PPIase intradomain restraints, which is optional.

^c Backbone (WW res6-39; PPlase 50–163), in parentheses only secondary structure elements (WW 8–15,23-27,31–33,35-39; PPlase 54–63,84-98,102–110,116-120,132–139,146-151,157–162).

Fig. 2. Agreement between experimental and back-calculated WW domain $^1D_{\text{Ni,HNi}}$ RDCs after structure calculation of the WW domain of Pin1. Plotted versus experimental RDCs are the RDCs back-predicted from a) the structure obtained by directly restraining the WW domain (step 1), and b, c) the structure obtained from the calculation using all restraints but freezing the WW domain angles (step 2). In a) and b) the alignment tensors were obtained from SVD on the WW domain, whereas in c) the alignment tensor was obtained from SVD on the PPlase with the PPlase domain $^1D_{\text{Ni,HNi}}$ RDCs. Pearson's correlation coefficients r are obtained from residues located in β-sheet only, or in any residue (all residues are plotted).

from both domains were utilized. We note that for such calculations the tensor of the more strongly aligned domain (in our case the PPIase domain is domain A) must be used for calculations using all RDCs, such that the more extensive RDC averaging of the less aligned domain (WW domain is domain B) will result in more diverse positions relative to domain A. All structure calculations (both for steps 1 and 2) were performed with 400 structures (in step 1 with random torsion angle values) using the standard simulated annealing protocol with 100,000 torsion angle steps. The conformer with the lowest TF from each of the 10 calculations was selected for the final ensemble (Table 1). Finally, we independently validated the obtained domain distributions, by comparing them to interdomain distances and their populations derived from DEER [33] measurements.

The structural ensembles resulting from steps 1 and 2 are shown in Fig. 1. The positions of the PPlase domain relative to the WW domain are shown in Fig. 1A after calculation of step 1. The structure of the WW is fully formed. Since we also applied restraints to the PPlase domain, some helices are already formed in the PPlase domain. As expected, the positions of the two PPlase states are typically far apart due to the absence of bundling restraints. After step 2, each conformer consisting of two simultaneously calculated states features an extended and a compact state (Fig. 1B), and both states have fully formed WW and PPlase domains.

An important question concerns the validity of the assumption made to derived equation (8) for the specific case of Pin1. Since the alignment induced by C12E5 PEG/hexanol is predominantly of steric nature, it is likely that both domains are affected by the alignment medium, which may compromise the validity of the approach. It is not possible to validate the approach with our data. However, a requirement is that the agreement between the measured WW domain RDCs and those back-calculated from the structures obtained from step 1 (equation (4)) and step 2 (equation (9)) should be similar. We tested this for $^{1}D_{\text{Ni,HNi}}$ RDCs. We made this choice because we use the experimental errors as tolerances for the RDCs in the structure calculation, within which the structures have to fulfill the measured RDCs. Therefore, the back-predicted RDCs are not forced to reproduce the input RDCs better than within the error. As a consequence, the correlation coefficients are less than what could be achieved from direct SVD fitting as mentioned above. Among all measured RDCs, $^{1}D_{\text{Ni,HNi}}$ have the smallest error relative to the measured range (0.64 Hz error for a range of 17.3 Hz).

Fig. 2 shows correlation plots of the measured and back-predicted RDCs after steps 1 and 2. Considering only the residues in the β sheet, Pearson's correlation coefficient even slightly increases from 0.86 to 0.89 when the alignment tensor for back-prediction is obtained from a *de novo* SVD on the WW domain. When the back-prediction is done using the alignment tensor from SVD to the PPlase domain instead, the correlation coefficient is virtually the same (0.87). Including all residues, the correlation coefficient slightly decreases from 0.88 after step 1 to 0.85 (WW alignment tensor) or 0.80 (PPlase alignment tensor) after step 2. Taken together, the values after steps 1 and 2 are comparable and therefore, the tested requirement for the validity of our approach is fulfilled for Pin1 under the used alignment condition.

The approach can be generalized to three or more domains. In the case of three domains, where A, B and C are the most, intermediate and least aligned domains, respectively, the first structure calculation would be carried out with domain C. The second step would involve freezing domain C and a structure calculation with the restraints both on domains B and C, but the alignment tensor from domain B. In the last step, both domains B and C would be frozen, and the restraints across all three domains would be applied, with the alignment tensor from domain A.

In conclusion, we introduced an approach to use RDCs in multi-state structures calculation such that we harvest not only intradomain but also interdomain geometry information inherent to the RDCs. Ideal alignment media would be those that directly induce alignment only on one domain, for example lanthanide tags, such that the assumptions made in equation (8) are strictly fulfilled.

Declaration of competing interest

The authors declare that they have no known competing financial interests or personal relationships that could have appeared to influence the work reported in this paper.

Acknowledgement

This project was supported by NIH Grant R01GM130694-01A1, a start-up package by the University of Colorado to B.V., University of Colorado Cancer Center Support Grant P30 CA046934, and NIH Biomedical Research Support Shared Grant S10 OD025020-01.

References

- [1] W. Wriggers, S. Chakravarty, P.A. Jennings, Control of Protein Functional Dynamics by Peptide Linkers. *Biopolymers Peptide Science Section*, John Wiley & Sons, Ltd January 1, 2005, pp. 736–746.
- [2] Y.E. Shapiro, NMR spectroscopy on domain dynamics in biomacromolecules, Prog. Biophys. Mol. Biol. (August 2013) 58–117.
- [3] C.A. Bewley, G.M. Clore, Determination of the relative orientation of the two halves of the domain-swapped dimer of cyanovirin-N in solution using dipolar couplings and rigid body minimization, J. Am. Chem. Soc. 122 (2000) 6009–6016.
- [4] D. Fushman, R. Varadan, M. Assfalg, O. Walker, Determining domain orientation in macromolecules by using spin-relaxation and residual dipolar coupling measurements, in: Progress in Nuclear Magnetic Resonance Spectroscopy, Elsevier July 30, 2004, pp. 189–214.
- [5] I. Bertini, Y.K. Gupta, C. Luchinat, G. Parigi, M. Peana, L. Sgheri, J. Yuan, Paramagnetism-based NMR restraints provide maximum allowed probabilities for the different conformations of partially independent protein domains, J. Am. Chem. Soc. 129 (2007) 12786–12794.
- [6] Y.E. Ryabov, D. Fushman, A model of interdomain mobility in a multidomain protein, J. Am. Chem. Soc. 129 (2007) 3315-3327.

- [7] J.J. Bouchard, J. Xia, D.A. Case, J.W. Peng, Enhanced sampling of interdomain motion using map-restrained Langevin dynamics and NMR: application to Pin1, J. Mol. Biol. 430 (2018) 2164–2180.
- [8] A. Born, J. Soetbeer, F. Breitgoff, M.A. Henen, N. Sgourakis, Y. Polyhach, P. Nichols, D. Strotz, G. Jeschke, B. Vögeli, Reconstruction of coupled intra- and interdomain protein motion from nuclear and electron magnetic resonance, J. Am. Chem. Soc. (2021), https://doi.org/10.1021/jacs.1c06289.
- [9] B. Vögeli, The nuclear overhauser effect from a quantitative perspective, Prog. Nucl. Magn. Reson. Spectrosc. 78 (2014) 1–46.
- [10] P. Nichols, A. Born, M. Henen, D. Strotz, J. Orts, S. Olsson, P. Güntert, C. Chi, B. Vögeli, The exact nuclear overhauser enhancement: recent advances, Molecules 22 (2017) 1176.
- [11] P.J. Nichols, A. Born, M.A. Henen, D. Strotz, C.N. Celestine, P. Güntert, B. Vögeli, Extending the applicability of exact nuclear overhauser enhancements to large proteins and RNA, Chembiochem 19 (2018) 1695–1701.
- [12] M. Karplus, J. Am. Chem. Soc. 85 (1963) 2870–2871.
- [13] J.L. Battiste, G. Wagner, Utilization of site-directed spin labeling and high-resolution heteronuclear nuclear magnetic resonance for global fold determination of large proteins with limited nuclear overhauser effect data, Biochemistry 39 (2000) 5879–5896.
- [14] G.M. Clore, Practical aspects of paramagnetic relaxation enhancement in biological macromolecules, Methods Enzymol. 564 (2015) 485-497.
- [15] N. Tjandra, A. Bax, Direct measurement of distances and angles in biomolecules by NMR in a dilute liquid crystalline medium, Science 278 (1997) 1111–1114.
- [16] J. Prestegard, H.M. Al-Hashimi, J.R. Tolman, NMR structures of biomolecules using field oriented media and residual dipolar couplings, Prog. Nucl. Magn. Reson. Spectrosc. 33 (2000) 371—424.
- [17] J.R. Tolman, K. Ruan, NMR residual dipolar couplings as probes of biomolecular dynamics, Chem. Rev. 106 (2006) 1720-1736.
- [18] B. Vögeli, P. Güntert, R. Riek, Multiple-state ensemble structure determination from eNOE spectroscopy, Mol. Phys. 111 (2013) 437–454.
- [19] G.M. Clore, C. Schwieters, J. Am. Chem. Soc. 126 (2004) 2923–2938.
- [20] J.A. Losonczi, M. Andrec, M.W.F. Fischer, J.H. Prestegard, Order matrix analysis of residual dipolar couplings using singular value decomposition, J. Magn. Reson. 138 (1999) 334–342.
- [21] K.P. Lu, S.D. Hanes, T. Hunter, A human peptidyl-prolyl isomerase essential for regulation of mitosis, Nature 380 (6574) (1996) 544-547.
- [22] M.B. Yaffe, M. Schutkowski, M. Shen, X.Z. Zhou, P.T. Stukenberg, J.U. Rahfeld, J. Xu, J. Kuang, M.W. Kirschner, G. Fischer, et al., Sequence-specific and phosphorylation dependent proline isomerization: a potential mitotic regulatory mechanism, Science (80-.) 278 (5345) (1997) 1957—1960.
- [23] A.T. Namanja, X.J. Wang, B. Xu, A.Y. Mercedes-Camacho, K.A. Wilson, F.A. Etzkorn, J.W. Peng, Stereospecific gating of functional motions in Pin1, Proc. Natl. Acad. Sci. 108 (30) (2011) 12289–12294.
- [24] R. Ranganathan, K.P. Lu, T. Hunter, J.P. Noel, Structural and functional analysis of the mitotic rotamase Pin1 suggest substrate recognition is phosphorylation dependent, Cell 89 (1997) 875–886.
- [25] D.M. Jacobs, K. Saxena, M. Vogtherr, P. Bernadó, M. Pons, K.M. Fiebig, Peptide binding induces large scale changes in inter-domain mobility in human Pin1, J. Biol. Chem. 278 (28) (2003) 26174–26182.
- [26] E. Bayer, S. Goettsch, J.W. Mueller, B. Griewel, E. Guiberman, L.M. Mayr, P. Bayer, Structural analysis of the mitotic regulator HPin1 in solution: insights into domain architecture and substrate binding, J. Biol. Chem. 278 (2003) 26183—26193.
- [27] P. Bernadó, M.X. Fernandes, D.M. Jacobs, K. Fiebig, J. García De La Torre, M. Pons, Interpretation of NMR relaxation properties of Pin1, a two-domain protein, based on brownian dynamic simulations, J. Biomol. NMR 29 (2004) 21–35.
- [28] J.W. Peng, Investigating dynamic interdomain allostery in Pin1, Biophys. Rev. 7 (2) (2015) 239–249.
- [29] P. Güntert, Automated structure determination from NMR Spectra, Eur. Biophys. J. 38 (2009) 129-143.
- [30] D. Strotz, J. Orts, H. Kadavath, M. Friedmann, D. Ghosh, S. Olsson, C.N. Chi, A. Pokharna, P. Güntert, B. Vögeli, et al., Protein allostery at atomic resolution, Angew. Chem. Int. Ed. 59 (2020) 2–10.
- [31] R. Ranganathan, K.P. Lu, T. Hunter, J.P. Noel, Structural and functional analysis of the mitotic rotamase Pin1 suggest substrate recognition is phosphorylation dependent, Cell 89 (1997) 875–886.
- [32] C.N. Chi, D. Strotz, R. Riek, B. Vögeli, Extending the ENOE data set of large proteins by evaluation of NOEs with unresolved diagonals, J. Biomol. NMR 62 (1) (2015) 63–69.
- [33] P.P. Borbat, E.R. Georgieva, J.H. Freed, Improved sensitivity for long-distance measurements in biomolecules: five-pulse double electron-electron resonance, J. Phys. Chem. Lett. 4 (2013) 170–175.



Beat Vögeli received B.S. and M.S. degrees in Physics and a Ph.D. degree in Physical Chemistry at ETH Zürich, Switzerland. After a postdoctoral stay at the National Institutes of Health, Bethesda USA, he returned to ETH Zürich to become Oberassistant and then Privatdozent. He is currently an assistant professor at the University of Colorado at Denver in the Department of Biochemistry and Molecular Genetics. He has expertise in NMR spectroscopy of proteins and nucleic acids, and develops methodology for the elucidation of their structures, dynamics and interactions.



Alexandra Born received her B.S. degrees in Chemistry and Biological Sciences: Microbiology from University of Rochester, and her Ph.D in Structural Biology and Biochemistry from the University of Colorado Anschutz. She is currently a post-doctoral scholar at the University of California San Francisco. She specializes in using NMR and other biophysical methods to discern conformational changes and alteration of dynamics in biological macromolecules.

ARTICLE IN PRESS

A. Born, M.A. Henen, P.J. Nichols et al.

Magnetic Resonance Letters xxx (xxxx) xxx



Morkos Henen. Morkos A. Henen received his Ph.D. degree in Molecular Biology at the University of Vienna, Austria. He was awarded a Marie Curie postdoctoral fellowship at the University of Lille, France. This was followed by postdoctoral training at the University of Pittsburgh, USA. Currently, he is a faculty research instructor at the University of Colorado, Denver, USA. He uses NMR and other biophysical techniques to study proteins/nucleic acids interactions and dynamics in addition to drug-discovery approaches.



Parker Nichols received a B.A. from Lewis and Clark College in Portland OR. He is currently working towards his Ph.D. in the labs of Dr. Beat Vögeli and Dr. Jeffrey Kieft in the Structural Biology and Biochemistry program at the University of Colorado at Denver. He uses NMR spectroscopy to investigate the dynamics and functions of proteins and nucleic acids.